

## STAGNATION POINT FLOW OF MHD WILLIAMSON NANOFLUID DUE TO NON UNIFORM HEAT SOURCE/SINK AND CHEMICAL REACTION OVER LINEAR STRETCHING SURFACE

*Yasin Abdela<sup>1</sup> & Bandari Shanker<sup>2</sup>*

<sup>1</sup>*Department of Mathematics, O.U, Hyderabad, India*

<sup>2</sup>*Professor, Department of Mathematics, University College of Science O.U, Hyderabad, India*

**Received: 09 May 2018**

**Accepted: 16 May 2018**

**Published: 04 Jun 2018**

### ABSTRACT

The numerical solution of stagnation point flow of MHD Williamson nanofluid with the effect of non-uniform heat source/sink and a chemical reaction over a linear stretching surface has been investigated. The governing partial differential equations have been transformed into a system of coupled ordinary differential equations by applying an appropriate similarity transformation. The most applicable numerical method that is the fourth order Runge-Kutta method along with shooting technique has been used to solve the systems of coupled ordinary differential equations. The influence of various parameters associated with the system of the ordinary differential equations such as the velocity ratio parameter  $\lambda$ , the magnetic field parameter, The Williamson parameter  $W$ , The chemical reaction parameter  $\gamma$ , the  $Pr$  and  $tl$  number  $Pr$ , the Schmidt number  $Sc$ , the Brownian motion parameter  $Nb$ , the thermophoresis parameter  $Nt$ , the space -dependent heat source/sink parameters  $A^*$  and temperature dependent heat source/sink parameter  $B^*$  are analyzed and graphically described. The skin friction  $C_f$ , the local Nusselt number  $Nu$ , the local Sherwood number  $Sh$ , were evaluated for different cases and investigated.

**KEYWORDS:** Linear Stretching Surface, Stagnation Point Flow, Williamson Nan Fluid, Non Uniform Heat Source/Sink and Chemical Reaction

### NOMENCLATURE

b	Velocity of the stretching surface
a	Free Stream velocity
T	Temperature of the fluid in the boundary layer
C	Concentration of the fluid in the boundary layer
$T_w$	Stretching surface temperature
$C_w$	Stretching surface concentration
$T_\infty$	Ambient fluid temperature
$C_\infty$	Ambient fluid concentration
u	Velocity component along the x- axis
v	Velocity component along the y- axis
$u_w$	Velocity component along the x- axis at the wall
$v_w$	Velocity component along the y- axis at the wall
$\nu$	Kinematic viscosity
$\tau$	The effective heat capacity of the Nano particle to the heat capacity of the fluid

$(\rho c)_p$	Effective heat capacity of Nano particle material
$(\rho c)_f$	Effective heat capacity of the Fluid
$\alpha$	Thermal diffusivity
$D_B$	Brownian diffusion coefficient
$D_T$	Thermophoresis diffusion coefficient
$k_1$	Thermal conductivity
$W$	Williamson parameter
$\gamma$	Chemical reaction parameter
$M$	Magnetic field parameter
$Pr$	Prandtl number
$Nb$	Brownian motion parameter
$Nt$	Thermophoresis parameter
$A^*$	The space dependent heat source/sink Parameter
$B^*$	The Temperature dependent heat source/sink Parameter
$Le$	Lewis number
$\lambda$	Velocity ratio parameter
$Cf_x$	Local skin friction
$Nu_x$	Nusselt number
$Sh_x$	Sherwood number

## 1. INTRODUCTION

Nanofluids are combinations of base fluids and nano sized (1-100 nm) particles (nanoparticles) dispersed within them. Examples of the base fluids are water; oil, glycol, polymeric solutions etc and the materials used for nanoparticles are like alumina, silica, diamond graphite,  $AlO_3$ , Cuo, Ag, and Cu. The advantages of Nanofluids are, it provides a high specific surface area and hence more heat transfer surface between particles and fluids, Nanofluids are more stable with sufficient viscosity, Nanofluids enhance thermophysical properties such as thermal conductivity, thermal diffusivity viscosity and convective heat transfer coefficient as compared to the base fluids.

The study of stagnation point flow of nanofluid over a linear stretching surface has many applications in technology and manufacturing industries. Some of them are saving power using nanofluid in closed loop cooling cycles, peristaltic pumps for diabetic treatments, in the extraction of Geothermal power nanofluids used to cool the pipes exposed to high temperature, solar collectors and nuclear applications, extrusion, melting spinning, the hot rolling; wire drawing, glass fiber production, manufacture of plastic and rubber sheets, cooling of a large metallic plate in bath, polymer sheets and filament are manufactured by continuous extrusion of the polymer from a die to a mind up roller etc.

Kavitha et al [1] have studied the peristaltic transport of a Williamson fluid in a symmetric channel through porous medium under the assumption of long wavelength and low Reynolds number. Jayarami et al [2] has investigated the MHD peristaltic flow of a Williamson fluid in a planar channel with the effect of Wiessenberg and Hartmann numbers. Vasudev et al [3] have examined the interaction of heat transfer with peristaltic pumping of a Williamson fluid through a porous medium in a planar channel under the assumption of low Reynolds number and long wavelength. Vitdal et al [4] have reported that the MHD stagnation point flow and heat transfer of Williamson fluid over exponentially stretching sheet embedded in a thermally stratified medium. Shiva et al [5] have presented the peristaltic flow of Williamson fluid in a vertical symmetrical channel with heat transfer under induced magnetic field and examined the effect of each parameter

involved. Sreenivasulu and Chakradhar [6] have dealt with the peristaltic flow of Williamson fluid between two porous walls with suction and injection under the assumption of low Reynolds number and long wavelength. Kumaran et al [7] have shown that the influence of melting heat transfer in MHD radioactive Williamson fluid flow past an upper paraboloid of revolution with viscous dissipation. Venkataramanaiah et al [8] studied the effect of the nano particles on the MHD boundary layer flow over a stretching surface in the presence of heat generation or absorption with heat and mass fluxes. Hasmawani et al [9] have investigated flow and heat transfer analysis of Williamson viscous fluid at the stagnation point over a stretching surface with viscous dissipation and slip condition. Iffat et al [10] have examined Williamson fluid with pressure dependent viscosity and determined numerical solutions. Sharada and Shankar [11] have reported that the effect of partial slip and convective boundary condition on the MHD mixed convection flow of Williamson fluid over an exponentially stretching sheet in the presence of joule heating. Ananthakumar et al [12] have presented the influence of thermal radiation and chemical reaction on MHD Williamson fluid over an exponentially stretching sheet. Khalid and Ahmed [13] have dealt with the influence of inclined magnetic field on the peristaltic flow of an incompressible Williamson fluid in an inclined channel with heat and mass transfer. Nagaraja et al [14] have explored heat transfer of Non Newtonian Williamson fluid flow past a circular cylinder with suction and injection. Bilal et al [15] have studied MHD Stagnation point flow of Williamson fluid over stretching cylinder with variable thermal conductivity and homogeneous – heterogeneous reaction. Shakhaoath et al [16] have reported the influence of magnetic field, thermal radiation-diffusion, heat generation and viscous dissipation on MHD flow of Williamson fluid. Krishnamurthy et al [17] have investigated the effect of chemical reaction on MHD boundary layer flow and melting heat transfer of Williamson nanofluid in porous media. Monica et al [18] have explored the stagnation point flow of a Williamson fluid over a non-linear stretching sheet with thermal radiation. Malik et al [19] have dealt with the effect of homogeneous-heterogeneous reaction in the Williamson fluid model over a stretching cylinder. Nagendra et al [20] have presented the slip effect on MHD flow of Williamson fluid from an isothermal sphere. Nabil et al [21] have reported the two dimensional motion of non Newtonian Williamson nanofluid with heat and mass transfer through the porous medium over an exponentially stretching sheet. Najeeb et al [22] have presented boundary layer flow of Williamson fluid with chemically reactive species using scaling transformation and homotopy analysis method. Nitta and Timol [23] have examined the invariance analysis of Williamson model using the method of satisfaction of asymptotic boundary conditions. Nadeem et al [24] have investigated the flow of a Williamson fluid over a stretching sheet. Nadeem and Hussain [25] have explored the two dimensional flow of Williamson fluid over a stretching sheet under the effect of nanosized particles in the fluid. Nadeem and Hussain [26] examined the effect of heat transfer on the Williamson fluid over a porous exponentially stretching the surface. Sreenadh et al [27] have reported the effect of slip and heat transfer on the peristaltic flow of a Williamson fluid in an inclined channel under long wavelength and low Reynolds number assumption. Subramanyam et al [28] have dealt with the fully developed free convection flow of a Williamson fluid through a porous medium in a vertical channel under the effect of magnetic field. Sirinivas et al [29] have studied the MHD boundary layer flow with heat and mass transfer of Williamson nanofluid over a stretching sheet with variable thickness and variable thermal conductivity under radiation. Hayat et al [30] have investigated the combined effects of Newtonian and joule heating in two dimensional flow of Williamson fluid over the stretching surface. Taza et al [31] have explored the thin film flow passed over an inclined moving plate with the differentiable type Non Newtonian Williamson is considered as a base fluid in its unsteady state.

The diversified application of nanofluids in different technologies and manufacturing industries enforced a number of investigators to conduct their research on the stagnation point flow of nanofluid over a linear stretching surface. However to the best of the author's knowledge the problem of stagnation point flow of MHD Williamson nanofluid due to non-uniform heat source/sink and chemical reaction over a linear stretching surface not yet explored. Therefore, in the present paper, the stagnation point flow of MHD Williamson nanofluid due to non-uniform heat source/sink and chemical reaction over a linear stretching surface has been investigated and reported.

## 2. MATHEMATICAL FORMULATION

We considered the steady two dimensional laminar stagnation point flow of incompressible Williamson nanofluid due to a linear stretching sheet. Assume that the velocity of the stretching sheet to be  $u_w(x) = bx$  and the velocity of the free stream flow to be  $U(x) = ax$ , where  $a, b$  are positive constants and  $x$  is the coordinate coinciding with the stretching sheet. The flow is conducted on the region  $y \geq 0$ , where  $y$  is the coordinate measuring orthogonal to the stretching sheet. Let,  $T_w, C_w$  be the temperature and concentration at the stretching sheet while  $T_\infty, C_\infty$  to be the ambient temperature and concentration of the nanofluid. And considered that the base fluid and the nano particles are in thermal equilibrium and no slips occur between them.

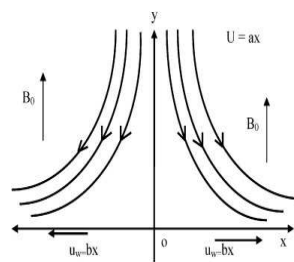


Figure 1: Physical Sketch of the Problem

In addition to the above assumptions we use the Williamson model as it is indicated in [29] to express the governing equations for the conservation of mass, momentum, energy and concentration as follows:

$$\frac{\partial u}{\partial x} + \frac{\partial v}{\partial y} = 0 \quad (1)$$

$$u \frac{\partial u}{\partial x} + v \frac{\partial u}{\partial y} = \nu \frac{\partial^2 u}{\partial y^2} + \sqrt{2\nu}\Gamma \frac{\partial u}{\partial y} \frac{\partial^2 u}{\partial y^2} - \frac{\sigma B_0^2 u}{\rho} + U \frac{\partial U}{\partial x} \quad (2)$$

$$u \frac{\partial T}{\partial x} + v \frac{\partial T}{\partial y} = \alpha \frac{\partial^2 T}{\partial y^2} + \tau \left[ D_B \frac{\partial C}{\partial y} \frac{\partial T}{\partial y} + \frac{D_T}{T_\infty} \left( \frac{\partial T}{\partial y} \right)^2 \right] + \frac{q'''}{\rho c_p} \quad (3)$$

$$u \frac{\partial C}{\partial x} + v \frac{\partial C}{\partial y} = D_B \frac{\partial^2 C}{\partial y^2} + \frac{D_T}{T_\infty} \frac{\partial^2 T}{\partial y^2} - k_0(C - C_\infty) \quad (4)$$

$q'''$  is the space and the temperature dependent heat source/sink that is defined as in [7]

$$q''' = \frac{k_1 u_w}{x\nu} [A^* (T_w - T_\infty) f' + B^* (T - T_\infty)] \tag{5}$$

The chemical reaction term  $k_0(C - C_\infty)$  as it is described in [16].

$u$  and  $v$  are the  $x$  and  $y$  direction, velocity components, respectively,  $\nu$  are the kinematic viscosity,  $\alpha$  is the thermal diffusivity,  $\tau$  is the effective heat capacity of nanoparticle to the heat capacity of the fluid,  $D_B$  is the Brownian motion coefficient,  $D_T$  is the thermophoresis diffusion coefficient,  $A^*$  and  $B^*$  are the parameters of the space and temperature dependent internal heat source/sink. If  $A^* > 0, B^* > 0$ , it represents heat is generated and  $A^* < 0, B^* < 0$  it represents heat is absorbed .

The corresponding boundary conditions are

$$\left. \begin{aligned} u = u_w = bx, \quad v = 0, \quad T = T_w, \quad C = C_w \quad \text{at } y = 0 \\ u = U(x) = ax, \quad T \rightarrow T_\infty, \quad C \rightarrow C_\infty \quad \text{as } y \rightarrow \infty \end{aligned} \right\} \tag{6}$$

The similarity transformation as it is indicated [24] is used to transform the partial differential equations to ordinary differential equations.

$$\left. \begin{aligned} \eta = \sqrt{\frac{b}{\nu}} y, \quad u = bx f'(\eta), \quad v = -\sqrt{\nu b} f(\eta) \\ \theta = \frac{T - T_\infty}{T_w - T_\infty} \quad \phi = \frac{C - C_\infty}{C_w - C_\infty} \end{aligned} \right\} \tag{7}$$

Applying (7) on (2), (3), (4) result in

$$\left. \begin{aligned} f'''' + Wf'' f'' + ff'' - f'^2 - M + \lambda^2 = 0 \\ \theta'' + Pr [Nb\phi'\theta' + \theta'f + Nt\theta'^2] + [A^* f' + B^* \theta] = 0 \\ \phi'' + Le \left[ \frac{Nt}{Nb} \theta'' + f\phi' - \gamma\phi \right] = 0 \end{aligned} \right\} \tag{8}$$

The corresponding boundary conditions are

$$\left. \begin{aligned} f'(0) = 1, \quad f(0) = 0, \quad \theta(0) = 1, \quad \phi(0) = 1 \quad \text{at } \eta = 0 \\ f \rightarrow \lambda, \quad \theta \rightarrow 0, \quad \phi \rightarrow 0 \quad \text{as } \eta \rightarrow \infty \end{aligned} \right\} \tag{9}$$

The primes are derivatives with respect to  $\eta$ , the velocity ratio parameter is  $\lambda = \frac{a}{b}$ , the magnetic field parameter

is  $M = \frac{\sigma\beta_0^2}{b}$ , the Williamson parameter is  $W = u\Gamma\sqrt{\frac{2b}{\nu}}$ , the prandtl number is  $Pr = \frac{\nu}{\alpha}$ , the Schmidt number is

$Le = \frac{\nu}{D_B}$ , the Chemical reaction parameter is  $\gamma = \frac{k_0}{b}$ , the Brownian motion parameter is  $Nb = \frac{D_B(C_w - C_\infty)}{(\rho_c)_f \nu}$  the

thermophoresis parameter is  $Nt = \frac{(\rho_c)_p D_T (T_w - T_\infty)}{(\rho_c)_f \nu T_\infty}$  and  $\tau = \frac{(\rho_c)_p}{(\rho_c)_f}$

It is known that Nb and Nt contains the x-coordinate and therefore it is must for us to search for the variability of the local similarity solution that allows us to investigate the behavior of these parameters at an affixed location above the sheet. The skin friction coefficient  $Cf_x$ , the local Nusselt number  $Nu_x$  and the local Sherwood number  $Sh_x$  are given by

$$Cf_x = \frac{\mu \left( \frac{\partial u}{\partial y} \right)_{y=0}}{\rho u_w^2}, \quad Nu_x = \frac{-x \left( \frac{\partial T}{\partial y} \right)_{y=0}}{T_w - T_\infty}, \quad Sh_x = \frac{-x \left( \frac{\partial C}{\partial y} \right)_{y=0}}{C_w - C_\infty} \quad (10)$$

Using the similarity transformation (7) on (10) we get

$$\text{Re}_x^{\frac{1}{2}} Cf_x = f''(0), \quad \frac{Nu_x}{\text{Re}_x^{\frac{1}{2}}} = -\theta'(0), \quad \frac{Sh_x}{\text{Re}_x^{\frac{1}{2}}} = -\phi'(0) \quad (11)$$

### 3. METHOD OF SOLUTION

The method used in the present paper is the numerical fourth order Runge-Kutta method along with shooting technique. To solve the coupled ordinary differential equations (8) with their corresponding boundary conditions (9) the Runge-Kutta method with shooting technique is employed. The system of nonlinear higher order differential equations (8) is changed into a system of first order differential equations in order to employ the method described. To transform the system of nonlinear higher order differential equations into a system of first order differential equations we apply the notations below.

Let

$$\left. \begin{aligned} f &= f(1), & f' &= f(2), & f'' &= f(3) \\ \theta &= f(4), & & & \theta' &= f(5) \\ \phi &= f(6), & & & \phi' &= f(7) \end{aligned} \right\} \quad (12)$$

Using equations (12) in equations (8) we have

$$\left. \begin{aligned}
 f''' + Wf''f''' + ff'' - f'^2 - M + \lambda^2 &= 0 \\
 \Rightarrow f''' &= -\frac{ff''}{1+Wf''} + \frac{f'^2}{1+Wf''} + \frac{M}{1+Wf''} - \frac{\lambda^2}{1+Wf''} \\
 \Rightarrow f''' &= -\frac{f(1)*f(3)}{1+W*f(3)} + \frac{f(2)*f(2)}{1+W*f(3)} + \frac{M}{1+W*f(3)} - \frac{\lambda^2}{1+W*f(3)}
 \end{aligned} \right\} \quad (13)$$

$$\left. \begin{aligned}
 \theta'' + \text{Pr}[Nb\phi'\theta' + \theta'f + Nt\theta'^2] + [A*f' + B*\theta] &= 0 \\
 \Rightarrow \theta'' &= -\text{Pr}[Nb\phi'\theta' + \theta'f + Nt\theta'^2] - [A*f' + B*\theta] \\
 \Rightarrow \theta'' &= -\text{Pr}[Nbf(7)f(5) + f(5)f(1) + Nt(f(2))^2] - [A*f(2) + B*f(4)]
 \end{aligned} \right\} \quad (14)$$

$$\left. \begin{aligned}
 \phi'' + Le\left[f\phi' - \gamma\phi + \frac{Nt}{Nb}\theta''\right] &= 0 \\
 \Rightarrow \phi'' &= -Le\left[f\phi' - \gamma\phi + \frac{Nt}{Nb}\theta''\right] \\
 \Rightarrow \phi'' &= -Le\left[f(1)f(7) - \gamma(6) - \frac{Nt}{Nb}\left[\text{Pr}(Nbf(7)f(5) + f(1)f(5) + Nt(f(2))^2) - A*f(2) - B*f(4)\right]\right]
 \end{aligned} \right\} \quad (15)$$

The boundary conditions are

$$\left. \begin{aligned}
 f_a(1) = 0, \quad f_a(2) = 1, \quad f_a(4) = 1, \quad f_a(6) = 1 \\
 f_b(2) \rightarrow \lambda, \quad f_b(4) \rightarrow 0, \quad f_b(6) \rightarrow 0 \\
 \text{where } a = 0 \quad \text{and } b = \infty
 \end{aligned} \right\} \quad (17)$$

The main objective is to change the boundary value problem into the initial value problem therefore we evaluate the approximate values of  $f''(0), \theta'(0)$  and  $\phi'(0)$  using the shooting technique first and then we apply the fourth order Runge-Kutta method to get  $f, \theta$  and  $\phi$ . We choose the step size to be  $\Delta h = 0.01$  with accuracy of  $10^{-5}$ .

#### 4. RESULTS AND DISCUSSIONS

The contribution of the distinct parameters intricate in the coupled ordinary differential equations such as the velocity ratio  $\lambda$ , the Williamson parameter  $W$ , the magnetic field parameter  $M$ , the prandtl number  $Pr$ , the Brownian motion parameter  $Nb$ , the thermophoresis parameter  $Nt$ , the space dependent and temperature dependent heat source/sink parameters respectively  $A^*$  and  $B^*$  and the Lewis number  $Le$ , the chemical reaction parameter  $\gamma$  on the stagnation point flow of Williamson nano fluid over a linear stretching surface have been examined with the help of their graphs and tabulated values.

**Table 1 Comparison Table of-  $\theta'(0)$  for Viscous Fluid with Different Values of Pr**

Pr	Khan & Pop	Nadeem & Hussian [25]	Present Result
0.2	0.169	0.169	0.16955
0.7	0.454	0.454	0.454448
2.0	0.911	0.911	0.911354

The present results for the considered prandtl number in table1 above agree to three decimal places with the results of Nadeem & Hussian [25]. Therefore the present results have excellent agreement with the results of the literature.

The velocity of the fluid and the boundary layer thickness escalated with the enlargement of the velocity ratio  $\lambda = \frac{b}{c} < 1$  (i.e. The velocity of the stretching surface is greater than the free stream velocity) as it is indicated in the first part of table 2. In the second part of table 2 below as the values of the Williamson parameter W enlarged from 0.01 to 0.03, the velocity of the fluid and the boundary layer thickness decreased. In the third part of table 2 the velocity and the boundary thickness diminished with the increment of the magnetic field parameter M due to the resistance force called Lorentz force. The Nusselt number increases as the prandtl number increase so that the thermal boundary layer thickness declines as it is shown in the fourth part of table 2. In the fifth, sixth, seventh and eight parts of table 2 enhancing Nb, Nt, A\* and B\* decreases the Nusselt number and thicken the thermal boundary layer because four of them contribute to the escalation of thermal energy of the nanofluid. In the 9<sup>th</sup> part of table 2, raising the chemical reaction parameter enhance the Sherwood number that depreciates the concentration boundary layer thickness. In the last part of table 2 the Nusselt number has diminished and the Sherwood number enlarges with the increase of Lewis number. As the Lewis number enlarges the molecular diffusivity becomes weaker and the concentration boundary layer thickness thinner.

**Table 2: The Values of -  $f''(0)$ ,  $-\theta'(0)$ ,  $-\phi'(0)$  for the Different Values of the Parameters**

$\lambda$	W	M	Pr	Nb	Nt	A*	B*	$\gamma$	Le	- $f''(0)$	- $\theta'(0)$	- $\phi'(0)$
0.2	0.001	0.01	1	0.01	0.01	0.01	0.01	0.1	3	0.932233	0.591916	1.075194
0.5										0.677630	0.658554	1.128082
0.8										0.308031	0.720607	1.185958
0.5	0.01	0.1	3	0.01	0.01	0.01	0.01	0.1	5	0.774969	1.183592	1.257602
	0.03									0.753607	1.189672	1.265562
	0.04									0.700485	1.204276	1.280356
0.1	0.05	0.01	3	0.01	0.01	0.01	0.01	0.1	5	0.850345	1.170849	1.255014
		0.03								0.921151	1.150828	1.235778
		0.04								0.929073	1.149000	1.234564
0.1	0.01	0.01	1	0.01	0.01	0.01	0.01	0.1	5	0.989480	0.567277	1.526832
			3							0.989480	1.124988	1.205206
			4							0.989480	1.324128	1.072596
0.1	0.01	0.01	1	0.1	0.01	0.01	0.01	0.1	5	0.989480	0.528305	1.701694
				0.2						0.989480	0.487746	1.71129
				0.3						0.989480	0.449934	1.714419
0.1	0.01	0.01	1	0.01	0.1	0.01	0.01	0.1	5	0.989480	0.544944	0.057087
					0.2					0.989480	0.521397	1.550604
					0.3					0.989480	0.499110	2.792375
0.1	0.01	0.01	1	0.01	0.01	0.1	0.01	0.1	5	0.989480	0.475868	1.579580
						0.2				0.989480	0.374254	1.638222
						0.3				0.989480	0.272587	1.696901
0.1	0.01	0.01	1	0.01	0.01	0.01	0.1	0.1	5	0.989480	0.476698	1.581604
							0.2			0.989480	0.349585	1.654961



**Table 2 Contd.,**

$\lambda$	W	M	Pr	Nb	Nt	A*	B*	$\gamma$	Le	$-f''(0)$	$-\theta'(0)$	$-\phi'(0)$
							0.3			0.989480	0.159735	1.757261
0.1	0.01	0.01	1	0.01	0.01	0.01	0.01	0.1	5	0.989480	0.567277	1.526832
								0.2		0.989480	0.567190	1.689784
								0.3		0.989480	0.567117	1.838297
0.1	0.01	0.01	1	0.01	0.01	0.01	0.01	0.1	3	0.989480	0.567795	1.059784
								6	0.989480	0.567123	1.721411	
								9	0.989480	0.566832	2.217055	

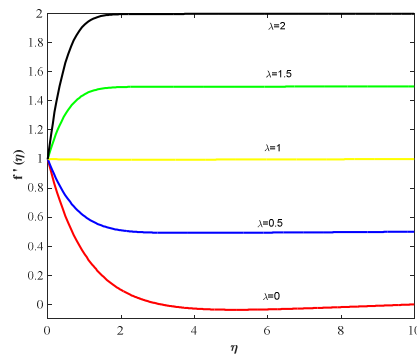


Figure 2: The Effect of the Velocity Ratio Parameter  $\lambda$  on the Velocity

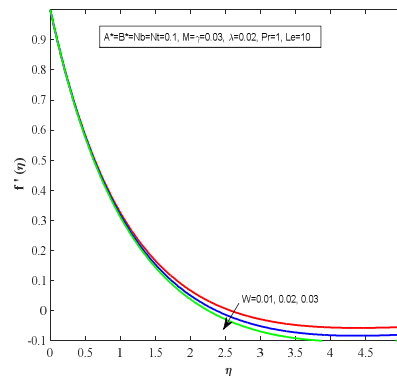


Figure 3: The Influence of the Williamson Parameter W of Velocity

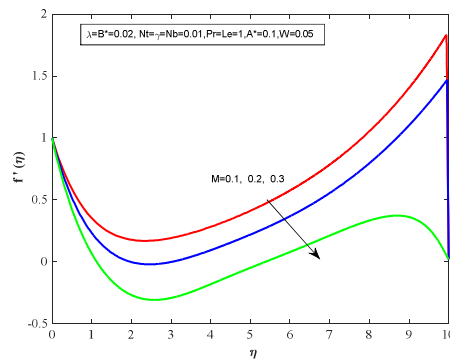


Figure 4: The Role of the Magnetic Field Parameter M on Velocity

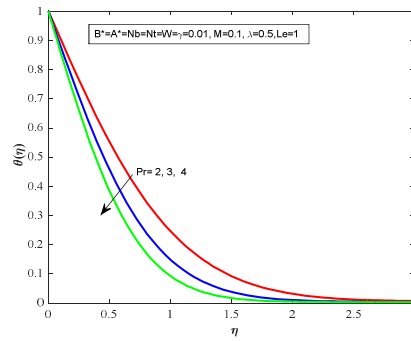


Figure 5: The Contribution of Pr on Temperature Profile

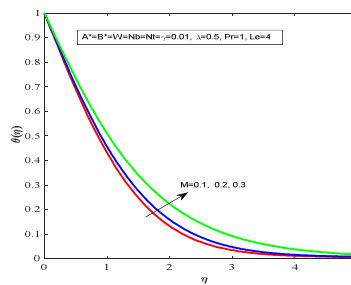


Figure 6: The Influence of the Magnetic Field Parameter M on Temperature Profile

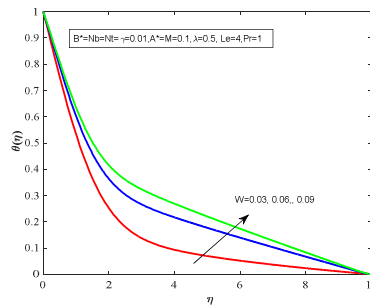


Figure 7: The Effect of the Williamson Parameter W on Temperature Profile

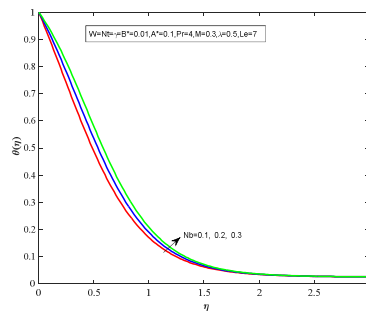


Figure 8: The Role of the Brownian Parameter NB on the Temperature Profile

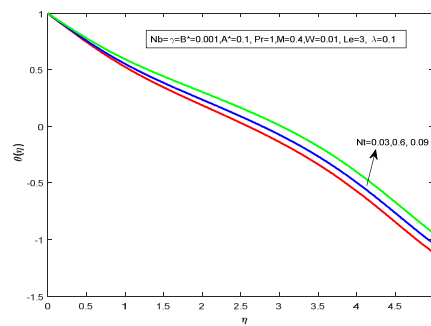


Figure 9: The Contribution of the Thermophoresis Parameter NT on Temperature Profile

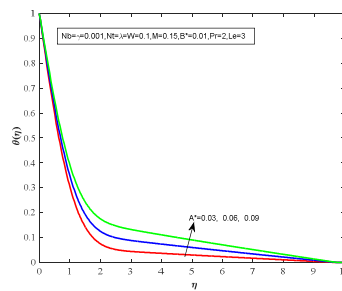


Figure 10: The Effect of A\* on the Temperature Profile

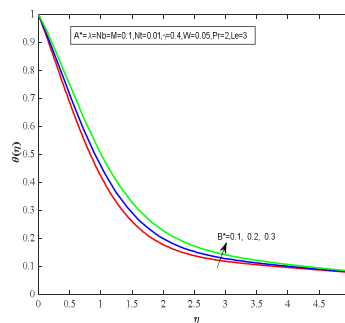


Figure 11: The Influence of B\* on Temperature Profile

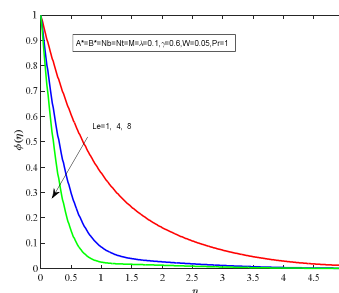


Figure 12: The Role of Le on the Concentration Profile

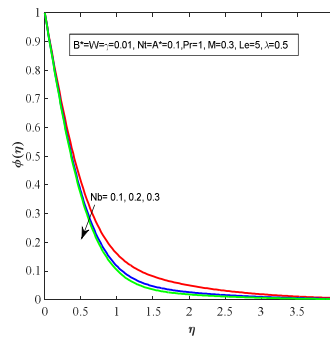


Figure 13: The Contribution of NB on the Concentration Profile

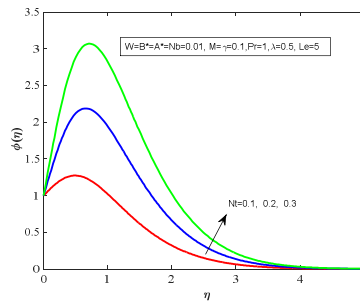


Figure 14: The Influence of NT on Concentration Profile

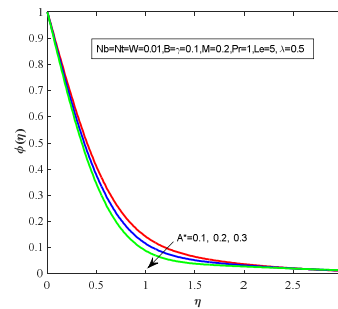


Figure 15: The Effect of A\* on Concentration Profile

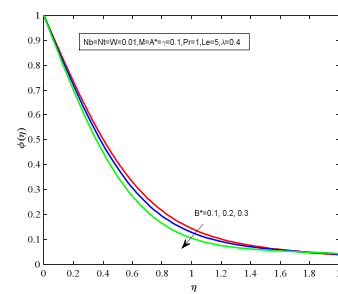
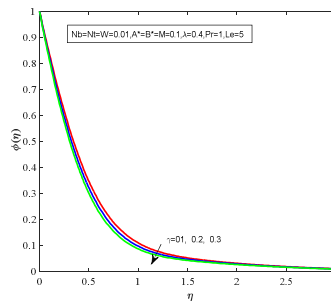


Figure 16: The Role of B\* on the Concentration Profile



**Figure 17: The Contribution of the Chemical Reaction Parameter  $\gamma$  on the Concentration Profile**

For  $\lambda = \frac{b}{a} < 1$  i.e. the velocity of the stretching surface is greater than the free stream velocity, the velocity of the

fluid and the boundary layer thickness enlarged with the upgrade of  $\lambda$ . To the contrary the flow velocity increases and the boundary layer thickness diminish with the enlargement of  $\lambda$  when the free stream velocity is larger than the velocity of the stretching surface (i.e.  $\lambda = \frac{b}{a} > 1$ ). In the third case where the two velocities are equal, there is no boundary layer thickness

of the nanofluid near the surface as it is revealed in Fig 2. Upgrading the Williamson parameter W declines the velocity as revealed in Fig3. Fig 4 elucidates that the influence of magnetic parameter on velocity. The velocity profile and the boundary layer thickness diminish with the upgrade of M. This is because of the Lorentz force that resists the motion of the fluid. The enhancement of the Prandtl number reduces the thermal boundary layer thickness. It is due to the smaller the thermal diffusivity the larger the Prandtl number as it is affirmed in Fig 5. The enlargement of the magnetic field parameter M and the Williamson parameter W magnifies the thermal boundary layer thickness as shown in Figs 6 and 7. The escalation in Brownian motion parameter and in thermophoresis parameter upgrades the thermal boundary thickness as it is depicted in Fig 8 and 9. This is because of the fact that the Brownian motion enforces more particles to move and gain more kinetic energy and hence the temperature profile enlarged and the thermophoresis diffusion enforces the nanoparticles to move from hot to cold flow regions which enlarges the thermal boundary layer thickness. In Figs 10 and 11, it is revealed that the thermal boundary layer thickness increases with the enlargement of the space and temperature dependent non uniform heat source/sink parameters  $A^*$  and  $B^*$  which corresponds to the internal heat generation that raises the temperature profiles. As the Lewis number enlarges the molecular diffusivity depreciates and the concentration boundary layer thickness becomes thinner as it is illustrated in Fig 12 so that as Le upgrades the concentration boundary layer thickness diminishes.

The concentration boundary layer thickness diminishes as the Brownian motion parameter escalated that is revealed in Figure 13, as Nb increases the Brownian motion enforces the nanoparticles transfers the surface heat to the fluid and the nanoparticles gain higher kinetic energy that contributes to the thermal energy of the fluid and causes the movement of the nanoparticles from hot to the cold region. However, the concentration boundary layer thickness increases with the increase of Nt as it is shown in Figure 14, increasing the thermophoresis diffusion creates fast movement of the nanoparticles from a region of high temperature to a region of low temperature. Figures 15 and 16 reveal that as the space - dependent  $A^*$  and the temperature dependent  $B^*$  heat source/sink parameters enhance, the concentration boundary layer thickness drops. Because as the nanofluid temperature increase with the increase of  $A^*$  and  $B^*$  diffusion of the

nanoparticles takes place from high to low-temperature regions and hence the concentration boundary layer decrease. Fig 17 shows that as the chemical reaction parameter escalated the concentration boundary layer thickness diminishes because of higher values of the chemical reaction parameter  $\gamma$  amount to a fall in the chemical molecular diffusivity.

### 3. CONCLUSIONS

The influence of chemical reaction, non-uniform heat source/sink, the magnetic field parameter, the Williamson parameter and the other parameters involved in the differential equations on the MHD Stagnation point flow of a Williamson nanofluid over a linear stretching surface has been studied. Numerical solutions of the governing equations are obtained that permit the computation of the flow, heat and mass transfer behaviors for various values of the velocity ratio  $\lambda$ , the Williamson parameter  $W$ , the magnetic field parameter  $M$ , the Prandtl number  $Pr$ , the Brownian motion parameter  $Nb$ , the thermophoresis parameter  $Nt$ , the non uniform heat source/sink space and temperature dependent parameters  $A^*$  and  $B^*$ , the chemical reaction parameter  $\gamma$  as well as the Lewis Number  $Le$  and we found that:

- The velocity boundary layer thickness enhances with the upgrade of the velocity ratio parameter,  $\lambda$  but depreciates with the magnetic field parameter  $M$  and the Williamson parameter  $W$ .
- The thermal boundary layer thickness diminishes with the enlargement of the Prandtl number
- The thermal boundary layer thickness magnifies with the upgrade of, Brownian motion parameter  $Nb$  and thermophoresis parameter  $Nt$ , the space-dependent  $A^*$  and temperature dependent  $B^*$  non-uniform heat source/sink .
- The escalation of the space dependent parameter ( $A^*$ ) and the Brownian motion parameter  $Nb$  declines the concentration boundary layer thickness.
- The concentration boundary thickness magnifies with the escalation of the thermophoresis parameter  $Nt$ .
- The concentration boundary thickness diminishes with the increase of the chemical reaction parameter  $\gamma$  and the Lewis number.

### REFERENCES

1. A.Kavitha I R. Hemadri Reddy S.Sreenadh I R.Saravana, *Peristaltic flow of a Williamson fluid in an asymmetric channel through porous medium. International Journal of innovative Technology and Creative Engineering, Vol. 1, NO. 1 2011.*
2. B. Jayarami Reddy, M.V Subba Reddy, C. Nadhamuni Reddy and P. Yogeswar Reddy *Peristaltic flow of a Williamson fluid in an inclined planar channel under the effect of magnetic field. Advances in Applied Science Research, 2012, 3 (1):452-461.*
3. C. Vasudev, Prof. U. Rajeswara Rao, M. V. Subba Reddy and G. Prabhakara Rao, *Peristaltic Pumping of Williamson fluid through a porous medium in a horizontal channel with heat transfer. American Journal of Scientific and Industrial Research, 2010, ISSN: 2153-649X doi:10.5251/ajsir.2010.1.3.656.666.*
4. Ch.Vittal, M. Chenna Krishna Reddy and T.Vijayalaxmi, *MHD Stagnation Point Flow and Heat Transfer of*

- Williamson Fluid over Exponential Stretching Sheet Embedded in a Thermally Stratified Medium. *Global Journal of Pure and Applied Mathematics*. ISSN 0973-1768 Volume 13, Number 6 (2017), pp. 2033-2056.
5. D. Shiva Kumar<sup>1</sup>, N. L. Bhikshu, M. V. Ramana Murthy, Y. V. K. Ravi Kumar, *Peristaltic Flow of a Conducting Williamson Fluid in a Vertical Asymmetric Channel with Heat Transfer through Porous Medium*. *IPASJ International Journal of Mechanical Engineering (IJME)*, Volume 3, Issue 8, August 2015.
  6. Dr. G. Sreenivasulu Reddy, Dr. K. Chakradhar, *Peristaltic Transport of a Williamson Fluid between Porous Walls with Suction and Injection*. *International Journal of Advanced Research in Science, Engineering and Technology*, Vol. 4, Issue 6, June 2017.
  7. G Kumaran, N Sandeep<sup>1</sup>, R Vijayaragavan, *Melting heat transfer in magneto hydrodynamic radiative Williamson fluid flow with non-uniform heat source/sink*. *IOP Conf. Series: Materials Science and Engineering* **263** (2017) 062022.
  8. G. Venkataramanaiah, Dr M.SreedharBabu, M.Lavanya, *Heat Generation/Absorption effects on Magneto-Williamson Nanofluid flow with Heat and Mass Fluxes*. *IJEDR | Volume 4, Issue 1 | ISSN: 2321-9939* *IJEDR1601061 International*, 2016
  9. Hasmawani Hashim, Muhammad Khairul Anuar Mohamed, Abid Hussanan, Nazila Ishak, Norhafizah Md Sarif<sup>5</sup>, Mohd Zuki Salleh, *Flow and Heat Transfer Analysis of Williamson Viscous Fluid on the Stagnation Point past a Stretching Surface with Viscous Dissipation and Slip Conditions*. *The National Conference for Postgraduate Research 2016, Universiti Malaysia Pahang*.
  10. Iffat Zehra, Malik Muhammad Yousaf, Sohail Nadeem, *Numerical solutions of Williamson fluid with pressure dependent viscosity*. *Results in Physics* 5 (2015) 20–25.
  11. K. Sharada and B. Shankar, *Effect of partial slip and convective boundary condition on MHD mixed convection flow of Williamson fluid over an exponentially stretching sheet in the presence of joule heating*. *Global Journal of Pure and Applied Mathematics*. ISSN 0973-1768 Volume 13, Number 9 (2017), pp. 5965-5975.
  12. K. Anantha Kumar, V. Sugunamma. J. V. Ramana Reddy and Sandeep, *Influence of Thermal radiation and chemical reaction on MHD Williamson fluid flow over an exponentially stretching sheet with suction*. *Open Journal of Applied & Theoretical Mathematics (OJATM)*, Vol. 2, No. 4, December 2016, and pp. 181 ~ 198.
  13. Khalid Al-Qaissy Ahmed M. Abdulhadi, *Effect of an Inclined Magnetic Field on Peristaltic Flow of Williamson Fluid in an Inclined Channel*. *Quest Journals Journal of Research in Applied Mathematics* Volume 3 ~ Issue 6 (2017) pp: 17-27.
  14. L. Nagaraja<sup>1</sup>, M. Sudhakar Reddy, M. Suryanarayna Reddy, *Heat Transfer of non-Newtonian Williamson Fluid Flow past a Circular Cylinder with Suction and Injection*. *International Journal of Innovative Research in Science, Engineering and Technology*, Vol. 6, Special Issue 13, July 2017.
  15. M. Bilal, M. Sagheer, S. Hussain, and Y. Mehmood, *MHD Stagnation Point Flow of Williamson Fluid over a Stretching Cylinder with Variable Thermal Conductivity and Homogeneous/Heterogeneous Reaction*. *Commun. Theor. Phys.* 67 (2017) 688–696

16. .Md. Shakhaoath Khana, Md. Mizanur Rahmana, b, S.M. Arifuzzamanc, Pronab Biswasc, Ifsana Karima, Williamson Fluid Flow behavior of MHD convective radiative cattaneo -Christov heat flux type over a linear stretched surface withheat generation and thermal diffusion. *Frontiers in Heat and Mass Transfer (FHMT)*, 9, 15 (2017).
17. M.R. Krishnamurthy, B.C. Prasannakumara, B.J. Gireesha, Rama Subba Reddy Gorla Effect of chemical reaction on MHD boundary layer flow and melting heat transfer of Williamson nanofluid in porous medium. *Engineering Scienceand Technology, an International Journal* 19 (2016) 53–61
18. Srinivas Maripala et al., Micropolar Nanofluid Flow over a MHD Radiative Stretching Surface with Thermal Conductivity and Heat Source/Sink, *International Journal of Mathematics and Computer Applications Research (IJMCAR)*, Volume 7, Issue 1, January-February 2017, pp. 23-34
19. M. Monica<sup>1</sup>, J. Sucharitha and Ch. Kishore Kumar, Stagnation Point Flow of a Williamson Fluid over a Nonlinearly Stretching Sheet with Thermal Radiation. *American Chemical Science Journal* 13(4): 1-8, 2016.
20. M. Y. Malik, T. Salahuddin, Arif Hussain, S. Bilal, and M. Awais, Homogeneous-heterogeneous reactions in Williamsonfluid model over a stretching cylinder by using Keller box method. *AIP Advances* 5, 107227 (2015).
21. [20] N. Nagendra, C.H. Amanulla., M. Sudhakar Reddy, Slip Effects on MHD Flow of a Williamson Fluid from an Isothermal Sphere: A Numerical Study. *AMSE JOURNALS-AMSE IETA publication-2017-Series: Modelling B; Vol. 86; N°3; pp 782-807.*
22. Nabil T. M. Eldabe<sup>1</sup>, Kawther A. Kamel<sup>2</sup>, Hamed M. Shawky<sup>2</sup> & Esmat A. Abd-Aziz, Flow of nano Williamson fluidwith heat and mass transfer through porous medium over an exponentially permeable stretching sheet. *IJRRAS* 34 (1) January 2018.
23. Najeeb Alam Khan, Sidra Khan and Fatima Riaz, Boundary Layer Flow of Williamson Fluid with Chemically Reactive Species using Scaling Transformation and Homotopy Analysis Method. *Math. Sci. Lett.* 3, No. 3, 199-205 (2014).
24. Nita Jain and M.G. Timol, Invariance Analysis of Williamson Model Using the Method of Satisfaction of Asymptotic Boundary Conditions. *International journal of Mathematics and scientific computing (ISSN: 2231-5330)*, Vol. 4, NO. 2, 2014.
25. S. Nadeem, S. T. Hussain and Changhoon Lee, Flow of Williamson Fluid over stretching sheet. *Brazilian Journal of Chemical Engineering*, Vol. 30, No. 03, pp. 619 - 625, July -September,.
26. S. Nadeem S. T. Hussain, Flow and heat transfer analysis of Williamson nanofluid, *Appl Nanosci* (2014) 4:1005–1012.
27. S. Nadeem, S. T. Hussain, Heat transfer analysis of Williamson fluid over exponentially stretching surface. *Appl. Math. Mech. -Engl. Ed.*, 35(4), 489–502 (2014).
28. S. Sreenadh, P. Govardhan, and Y. V. K. Ravi Kumar, Effects of Slip and Heat Transfer on the Peristaltic Pumping of a Williamson Fluid in an Inclined Channel. *Int. J. Appl. Sci. Eng.*, 2014. 12, 2 143.



29. S. Subramanyam, M. V. Subba Reddy and B. Jayarami Reddy, Influence of Magnetic Field on Fully Developed Free Convective Flow of a Williamson Fluid through a Porous Medium in a Vertical Channel. *Journal of Applied Mathematics and Fluid Mechanics*, Volume 5, Number 1 (2013), pp. 33-44.
30. Srinivas Reddy, Kishan Naikoti, Mohammad Mehdi Rashidi, MHD flow and heat transfer characteristics of Williamson nanofluid over a stretching sheet with variable thickness and variable thermal conductivity. *Transactions of A. Razmadze Mathematical Institute* 171 (2017) 195–211.
31. T. Hayat, A. Shafiq, M. A. Farooq, H. H. Alsulami and S. A. Shehzad, Newtonian and Joule Heating Effects in Two- Dimensional Flow of Williamson Fluid. *Journal of Applied Fluid Mechanics*, Vol. 9, No. 4, pp. 1969-1975, 2016.
32. Taza Gul I, Abdul Samad Khan, Saeed Islam, Aisha M. Alqahtani, Ilyas Khan, Ali Saleh Alshomrani, Abdullah K. Alzahrani and Muradullah, Heat Transfer Investigation of the Unsteady Thin Film Flow of Williamson Fluid Past an Inclined and Oscillating Moving Plate. *Appl. Sci.* 2017, 7, 369.

